Soft Matter

Accepted Manuscript

ROYAL SOCIETY OF CHEMISTRY

www.rsc.org/softmatter

Hydrodynamic instability in magnetically driven suspension of paramagnetic red blood cells

B. E. Kashevsky, A. M. Zholud, S. B. Kashevsky

A.V. Luikov Heat and Mass Transfer Institute, National Academy of Sciences of Belarus. P. Brovka str. 15, Minsk, 220072, Belarus. E-mail: bekas@itmo.by

We address magnetically driven motion in suspensions of paramagnetic particles. Our object is diluted deoxygenated whole blood with paramagnetic red blood cells (RBCs). We use direct observations in a closed vertical Hele-Shaw channel, a well-defined magnetic force field applied horizontally in the channel plane. At very low cell concentration we register single-particle motion mode, track individual cells and determine their hydrodynamic and magnetic characteristics. Above 0.2 volume percent concentration we observe local swirls and global transient quasi-periodic vortex structure intensifying with increasing cell concentration but surprisingly not influencing time and purity of RBCs magnetic extraction. Our observations shed light upon behavioral complexity of magnetically driven submagnetic suspensions, an issue, important for the emerging microfluidic technology of direct magnetic cell separation and intriguing for mechanics of particulate soft matter.

Collective hydrodynamic effects in suspensions of driven particles represent a long-standing problem in fluid mechanics and statistical physics[1], their understanding to be of essential importance to a range of traditional industries and sophisticated modern applications. Recently, in relation with the emerging diagnostic applications of microfluidic analytical systems, much attention has been drawn[2] by the old tempting idea[3] of magnetically driven separation of submagnetic microparticles, especially biological particles, with the use of their intrinsic magnetic differences and high-gradient magnetic fields. The immediate subject of these studies is blood which is extensively used for diagnostics, and which is known for the noticeable among biological matters difference in magnetic susceptibilities of the white and the deoxygenated red blood cells whose hemoglobin iron is in high-spin paramagnetic state. Nevertheless, magnetic force that can be applied to RBCs in microfluidic systems is relatively small, so that efficient magnetic schemes of cell manipulation became the main concern of current studies, their conception not going beyond the single-particle motion theory.

In this communication we present first experimental evidence of intricate cooperative behavior in magnetically driven suspension of deoxygenated RBCs, and formulate its basic

physical conception. First of all, as opposed to suspensions of ferromagnetic particles (such as magnetic fluids[4] and magnetorheological fluids[5]), in case of submagnetic suspensions it is possible to rule out both local (interparticle) and global (caused by the self-magnetic fields of the test subjects) cooperativity of magnetic origin. This means that the motion of particles proceeds at a given magnetic force field and points at the similarity between magnetic separation and gravity sedimentation, which collective nature is of hydrodynamic origin and remains in focus of fluid mechanics for long years[1], including, particularly, sedimentation in confined microfluidic conditions[6]. Thanks to the possibility of controlling the driving force intensity and configuration, magnetic sedimentation represents an intriguing subject for this brunch of science.

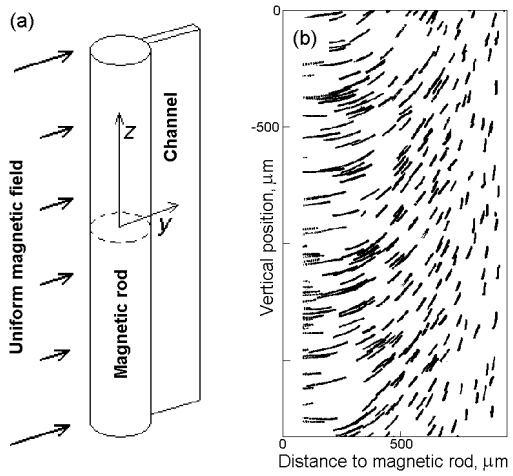

Fig.1 Schematic of measuring microfluidic cell (a), and trajectories of RBC in sample S1.5 (b).

To study magnetically driven suspensions at both single-particle and macroscopic scales we use quasi two-dimensional experimental model that ensures simple deterministic conditions, visualization, and, in case of dilute suspensions, tracking of individual cells. Our experimental setup is the slightly modified magnetophoretic trajectory-tracking magnetometer recently developed for accessing magnetic properties of submagnetic microparticles and cells[7]. The suspension sample is confined in a slot vertical rectangular channel with its depth (0.12 mm) much smaller than the width ($W = 0.96$ mm) and the width much smaller than the height (20 mm). The motion proceeds under the action of the mutually perpendicular (in the channel plane) gravity and magnetic force fields. The latter is created by a soft-magnetic cylindrical rod that abuts against one of the vertical channel edges and is magnetized (magnetization $I = 1210$ emu/cm^3) by the uniform horizontal magnetic field with intensity $H_0 = 9600$ Oe applied in the channel plane (Fig. 1a). The rod diameter (1mm) is small as against the channel height and large as against the channel depth, so that the driving magnetic force, except for the border regions

near the rod ends, is directed horizontally in the channel plane, is uniform along its both high and depth, and has a simple analytical representation[7], which makes this model fit for experimental and theoretical studies. The observation can be done both inside and outside magnetic field. The sample is delivered into the channel by a microhydraulic system (see ref. 7), its outlet being sealed prior to the registration to set the suspension as a whole motionless. Experiments are performed with suspensions prepared by diluting fresh fingertip blood of one of the authors with the pharmaceutical saline solution (+ 2% of serum albumin), followed by a 40 min blowing-off each sample, in a sealed slightly rocking penicillin battle, with nitrogen. The overwhelming majority of observable cells are RBSs, the white cells are as rare as one in a million. The 2.5 mm high observation area is situated half way along the channel, the digital microscope with the pixel size of 2.55x2.55 μm gives clear display of red and white cells, and shadows of the platelets. In this very first study, we put aside the detailed mesoscopic motion characterization, and deal mainly with the global behavior.

To provide a primary theoretical background, consider suspension of cells as a two-phase continuum with known physical properties of its constituents (ρ_0, ρ and χ_0, χ to be the liquid and the cell densities and magnetic susceptibilities, η_0 to be the liquid viscosity, and V, the cell volume), and with a given initial volume concentration of cells c_0. To describe the system dynamics, we use the local macroscopic characteristics of the disperse phase (the concentration c, and the velocity $\mathbf{w}$ of cells), and of the suspension as a whole (the density $\rho_s = c\rho + (1-c)\rho_0$, the magnetic susceptibility $c\chi + (1-c)\chi_0$, the mass velocity $\mathbf{u}$, the effective viscosity η, and the hydraulic pressure P). In accordance with the electrodynamics of continuous media[8], a nonuniform magnetic field exerts on liquid and cells the magnetic body forces with densities $\chi_0 \nabla\left(H^2/2\right)$ and $\chi\nabla\left(H^2/2\right)$ respectively. In the stationary liquid, the magnetic body force is compensated by the additional fluid pressure which creates the additional (magnetic) buoyancy force $-\chi_0 V\nabla\left(H^2/2\right)$. Further on, we keep to the usual for Hele-Shaw problems approach[9], and consider the suspension motion as effectively two dimensional with locally plane Poiseuille velocity profile. This leads to the following equation for the averaged over the channel depth suspension velocity $\left(\Delta\rho = \rho - \rho_0, \quad \Delta\chi = \chi - \chi_0\right)$:

$$\mathbf{u} = \frac{h^2}{12\eta}\left(-\nabla p + c\Delta\rho\mathbf{g}_0 + \frac{1}{2}c\Delta\chi\nabla H^2\right). \qquad (1)$$

In this equation we have excluded the hydrostatic pressure $P_0 = const + \mathbf{r}\cdot\mathbf{g}_0 + \chi_0 H^2/2$ ($\mathbf{g}_0$, the gravity vector), existing in the stationary liquid without cells, $p = P - P_0$. For the 2D velocity of cells driven by the gravity and the magnetic force, with inclusion of the related buoyancies, we write

$$\mathbf{w} = \mathbf{u} + \beta(\tilde{n})\left[\Delta\rho\mathbf{g}_0 + \frac{1}{2}\Delta\chi\nabla H^2\right]. \qquad (2)$$

Egn. (2) extends the gravity sedimentation equation to account for the additional (magnetic) driving force, the macroscopic mobility of cells, $\beta(c)$, is taken velocity-independent excluding the possibility of hydrodynamic deformation of RBCs during their magneto-gravitational sedimentation. We accept the macroscopic mobility function in the form of the widely used empirical relation[10] $\beta(c) = \beta_0(1-c)^k$ with $k \approx 4.7$, the coefficient β_0 representing the single-cell mobility, averaged over its random orientations. The formulation is completed by the equations representing the mass conservation law for the suspension and the cells:

$$\nabla\cdot\mathbf{u} = 0, \quad \frac{\partial\tilde{n}}{\partial t} + \nabla\cdot(c\mathbf{w}) = 0. \qquad (3)$$

The first Eqn. (3) is derived from the general continuity equation for suspension,

$$\frac{\partial\rho_s}{\partial t} + div\,\rho_s\mathbf{u} = 0.$$

With account of $\rho_s = c\rho + (1-c)\rho_0$ it gives relation

$$div\mathbf{u} = -\frac{\Delta\rho}{\rho_0}\left(\frac{\partial c}{\partial t} + divc\mathbf{u}\right),$$

from which the first Eqn. (3) follows as the first-order approximation, the right-hand term substituted by zero, given $\Delta\rho/\rho_0 << 1$ and $c << 1$.

Considering the system behavior in the middle part of the channel (far from its top and bottom), we indicate the basic motion mode in which magneto-gravitational sedimentation of cells proceeds height-independently, $c = c(y,t)$, accompanied by a zero-discharge vertical flow of the suspension originated by the nonuniform time-varying distribution of cell concentration (hence, the suspension density) along the channel width. For this state, in the planar coordinate system of Fig. 1a, the above equations give

$$u_y = 0, \quad u_z = \left(h^2 \Delta\rho g_0 / 12\eta_s\right)\left(\overline{c} - c\right), \tag{4a}$$

$$p = const - \Delta\rho g_0 \overline{c} z + \left(1/2\right) c\Delta\chi H^2, \tag{4b}$$

$$w_z = u_z - \Delta\rho g_0 \beta_0 \left(1-\tilde{n}\right)^k, \tag{4c}$$

$$w_y = \frac{1}{2}\beta_0 \Delta\chi \left(1-\tilde{n}\right)^k \frac{dH^2}{dy}, \tag{4d}$$

$$\frac{\partial c}{\partial t} + \frac{\partial}{\partial y}\left(c w_y\right) = 0 \tag{5}$$

It should be pointed out that these equations, as well as Eqns. (1)-(3), do not describe the sediment layer built up on the lateral channel walls. The magnetically settled cells just disappear from the channel, the quantity $\overline{c}$ in Eqns. (4a) representing the averaged over the channel width concentration of the remaining cells.

The driving magnetic force field in Eqn. (4d) is given by the relation[7]

$$\frac{1}{2}\frac{dH^2}{dy} \equiv f = -\frac{4\pi H_0 I}{R}\left[\left(\frac{R}{y}\right)^3 + \frac{2\pi I}{H_0}\left(\frac{R}{y}\right)^5\right]. \tag{6}$$

Here R is the magnetic road radius. An important analytical result from the motion equation (4d) is the overall separation time, T, in the single-particle approximation. This is the time for cells to cross the whole channel, for which Eqn. (5) with $k = 0$ yields

$$T = \frac{R^2 \beta_0 |\Delta\chi|}{4\pi H_0 I}\left[S\left(1 + \frac{W}{R}\right) - S\left(1\right)\right]. \tag{7}$$

Here

$$S\left(\zeta\right) = \frac{\zeta^4}{4} - \frac{\pi I}{H_0}\frac{\zeta^2}{2} + 2\left(\frac{\pi I}{H_0}\right)^2 \ln\left(\zeta^2 + \frac{2\pi I}{H_0}\right).$$

The number concentration of cells in the studied samples amounted to 1.5, 3, 6, 12, 24, 48, 100 and 250 thousands per cmm. The corresponding volume concentration, estimated as $c = nV$, $V = 9\cdot 10^{-8}$ mm^3 to be the mean volume of RBCs, was in the range from 0.00014 to 0.023. In the undiluted blood $n = 5\cdot 10^6$ mm^{-3}, $c \approx 0.45$. Different concentration samples are denoted by the symbol Sn, n stays for the number concentration of cells (in thousands per cmm).

In very dilute suspensions (up to $n = 12 \cdot 10^3$ mm^{-3}) the pattern of the process is in compliance with the above described basic mode, the video processing software[7] allowing tracking individual cells up to $n = 6 \cdot 10^3$ mm^{-3}. The registered trajectories of cells in sample S1.5 are presented in Fig. 1b. As the vertical-to horizontal displacements ratio of moving cell at a small time interval (local trajectory inclination) reflects the gravity-to magnetic force ratio, Fig.1b tells that the driving magnetic force is much stronger than the driving gravity force in the magnetic rod vicinity and rapidly drops on moving away from the rod. From the measured mean vertical velocity of cells in this sample, $w_z = -1.53$ μm/c, accepting the mean RBC density $\rho = 1.09$ g/cm^3, and the measured density of the liquid carrier $\rho_0 = 1.005$ g/cm^3 ($\Delta\rho = 0.085$ g/cm^3), we find the mean single cell mobility $\beta_0 = |w_z| / g_0 \Delta\rho = 1.834 \cdot 10^{-6}$ c·cm/g. Using the trajectory tracking technique of ref. 7 we also obtain the mean relative specific magnetic susceptibility of cells, $\kappa = \Delta\chi / \Delta\rho = 2.1 \cdot 10^{-6}$ cm^3/g, and find their mean magnetic susceptibility $\Delta\chi = 1.79 \cdot 10^{-7}$. For the magnetic-to gravity force ratio $\kappa f / g_0$, with the use of Eqn. (6) we find the value of 11.2 at the magnetic rod surface, of 0.94 in the middle of the channel, and of 0.25 at its remote edge. Also, with the actual characteristics of the system evaluated, Eqn. (7) gives the total separation time $T = 13.5$ min. Indeed, after this time inside magnetic field, there are just several cells left in the channel, most of them white blood cells. Moreover, numerical solution of Eqns. (4d, 5, 6) gives the time-varying cell distribution which is in good agreement with measurements performed in very diluted suspensions. Here we skip these data for the sake of a more interesting cooperative phenomenon arising as the cell concentration increases, its precondition to be the above mentioned peculiarity of magnetic attraction of RBCs toward magnetic rod: strong near the rod and rapidly decreasing on moving away from it.

To illustrate our observations in more concentrated suspensions we use the snapshots of the time-varying cell distribution (Fig. 2), and the maps of short-time tracks of moving cells (Fig.3). The latter we obtain by processing of the original videos that includes first grayscale and then binary conversion (by appointing the gray image points, using an appropriate intensity level, to either cells (intensity 1) or the background (intensity 0), followed by compositing four successive frames taken in 1 c intervals. Increasing cell concentration exposes clearly an important peculiarity of the process: a relatively rapid cell depletion of the magnetic rod-adjacent region creates rather step invert stratification of cell concentration (Fig. 2). In the stratified region, the first obvious deviation from the basic state appears at still rather low initial concentration ($n = 24 \cdot 10^3$ mm^{-3}, $c = 0.0022$) in the form of large-scale, quasi-periodic along the channel height, granular structure (Fig. 2). The cell tracking maps in this sample (Fig. 3b,c) show the global vertical flow and the accelerated horizontal motion of cells within more concentrated

regions. This indicates the born quasi-periodical hydrodynamic vortex structure. The descending (toward magnetic rod) suspension brings cells from the more concentrated remote part of the channel, while the ascending suspension is depleted of cells pulled out on passing the near-rod area. Noteworthy is the spotty velocity/concentration pattern (Fig. 3b) developed prior to the global instability. The intensity of the hydrodynamic motion increases with increasing cell concentration (Fig. 3e,f) bringing about the intricate swirling structure with flow velocity far exceeding that of single cell magnetophoresis (Fig. 3f,g,h). Point out that the spatial scale (about 1 mm) of this quasi-periodic structure does not depend on the cell concentration (Fig. 3 c,e,g) and should be related with the scale of the magnetic field nonuniformity, the magnetic rod diameter.

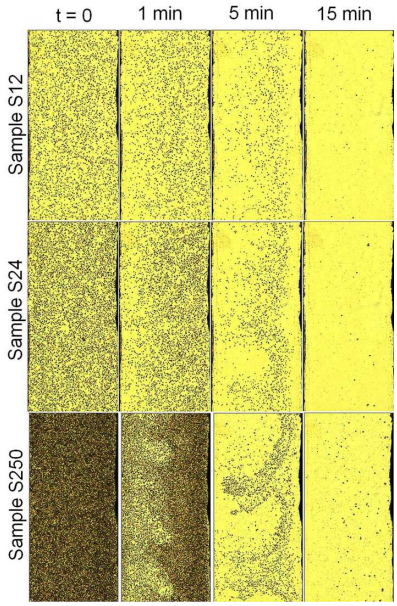

Fig. 2 Snapshots of the time-varying cell distribution in samples of different concentration

Fig. 3 Maps of 3-second tracks of moving cells in different-concentration samples

A surprising result of our observations is that the vigorous hydrodynamic agitation, at least up to the largest studied concentration $c = 0.023$, does not affect the overall separation time of RBCs. This fact is illustrated by Fig. 2 showing just a few cells left in the channel after 15 minutes in different-concentration suspensions. The remaining cells, moving in the opposite direction, are diamagnetic white cells, and their counting gives the numbers proportional to the initial number concentration of cells, signifying that the hydrodynamic entrainment of white cells, in the studied range of concentrations, does not affect the separation purity of RBCs.

Theoretical analysis of the observed granular magnetophoretic instability represents a challenging problem, unusual for hydrodynamics. Its peculiarity is the absence of a steady motion state, the magnetic sedimentation process to be entirely transient, the introduced basic state equations not having analytical solution, on which perturbations could be imposed. The understanding of the true nature of the hydrodynamic instability, which clear signs appear in sample S24 with the mean distance between cells, $n^{-1/3} \approx 35$ μm, only about 3 times smaller than the channel depth, may need more complicated consideration with account for the interplay between mesoscopic (interparticle) and macroscopic hydrodynamics, an important issue of the driven suspension mechanics.

In conclusion, our observations shed light upon behavioral complexity of magnetically driven submagnetic suspensions, an issue, important for the emerging microfluidic technology of direct magnetic cell separation and intriguing for mechanics of particulate soft matter.

Supported by State Program of Scientific Research “Interdisciplinary studies and arising technologies”, task 3.2.03.

References

1. G. K. Batchelor and J. T. Green, *J. Fluid Mech.* 1972, **56**, 401; S. Ramaswamy, *Advances in Physics* 2001, **50**, 297; H. Löwen, *Soft Matter* 2010, **7**, 3133; É. Guazzelli and J. Hinch, *Ann. Rev. Fluid Mech*. 2011, **43**, 97.

2. E. P. Furlani, *J. Phys. D: Appl. Phys*. 2007, **40,** 1313; J. Jung and K. Han, *Appl. Phys. Lett.* 2008, **93**, Art. No 223902; D. R. Gossett, W. M.Weaver, A. J.Mach, S. Claire Hur, H. Tat. K. Tse, W. Lee, H. Amini and D. Di Carlo, *Analytical and Bioanalytical Chemistry* 2010, **379**, Art. No 3249; Y. Jung, Y. Choi, K. Han and A. B. Frazier, *Biomedical Microdevices* 2010, **12**,637; L. R. Moore, F. Nehl, J. Dorn, J. J. Chalmers and M. Zborowski, *IEEE Trans. on Magn*. 2013, **49**, 309; J. Nam, H. Huang, H. Lim, C. Lim and S. Shin, *Anal. Chem.* 2013, **85**, 7316**.**

3. S. J. Gill, C. P. Malone and M. Downing, *Rev. Sci. Instrum.* 1960, **31**, 1299; D. Melville, F. Paul and S. Roath, *Nature*1975, **255**, 706; C. S. Owen, *Biophys. J.* 1978, **22**, 171; F. Paul, S. Roath, D. Melville, D. C. Warhurst and J. O. S. Osisanya, *Lancet* 1981, **2**, 70

4. R. E. Rosensweig, *Ferrohydrodynamics* (Cambridge University Press, Cambridge, 1985).

5. J. de Vicente, D. J. Klingenberg and R. Hidalgo-Alvarez, *Soft Matter* 2011, 7, 3701.

6. A. Wysocki, C. P. Royall, R. G. Winkler, G. Gompper, H. Tanaka, A. van Blaaderen and H. Löwen, *Soft Matter* 2009, **5**, 1340; M. J. Niebling, E. G. Flekkoy, K. J. Maloy and R. Toussaint, *Phys. Rev. E* 2010, **82**, Art. No 051302; N. Desreumaux, J.-B.Caussin, R. Jeanneret, E. Lauga and D. Bartolo, *Phys. Rev. Lett.* 2013, **111**, Art. No118301.

7. B.E. Kashevsky, A. M. Zholud and S. B. Kashevsky, *Rev. Sci. Instrum.* 2012, **83**, Art. No 075104.

8. L. D. Landau and E. M. Lifshitz, *Electrodynamics of Continuous Media* (Pergamon, New York, 1959).

9. D. Bensimon, L. P. Kadanoff, S. Liang, B. I. Shraiman and C. Tang, *Rev. Modern Phys.* 1986, **58**, 977.

10. R. Di Felice and R. Kehlenbeck, *Chem. Eng. Technol*. 2000, **23**, 1123.

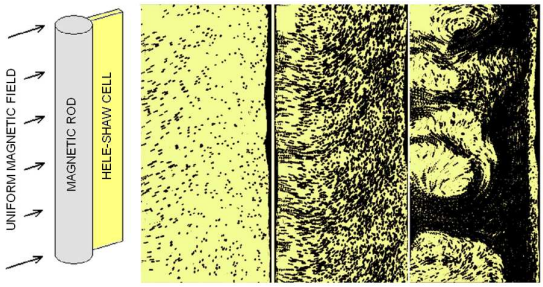

Visualization of magnetically driven paramagnetic red blood cells in Hele-Shaw channel reveals transition from single-particle to collective motion mode as the cell concentration increases